

# Effect of Airborne Pathogen Transmission Released by an Assailant in A Mosque Using CFD Simulation

Mohamad Nur Hidayat Mat<sup>1\*</sup>, Muhammad Faizal Azman<sup>1</sup>, Eliza M. Yusup<sup>2</sup>

<sup>1</sup>Faculty of Mechanical Engineering,  
Universiti Teknologi Malaysia, 81310 UTM Johor Bahru, Johor, MALAYSIA

<sup>2</sup>Bioactive Material (BIOMA), Fakulti Kejuruteraan Mekanikal dan Pembuatan,  
Universiti Tun Hussein Onn Malaysia, 86400 Parit Raja, Johor, MALAYSIA

\*Corresponding Author

DOI: <https://doi.org/10.30880/ijie.2023.15.04.012>

Received 22 May 2022; Accepted 14 May 2023; Available online 28 August 2023

**Abstract:** This study investigated the aerosol particle spreading characteristic under transient state at different location released by an assailant inside a mosque. Particles deposited at receivers were used to determine the virus reproductive number ( $R_0$ ) over time. The spreading during coughing process was validated with previous literature review using Computational Fluid Dynamics (CFD) simulation study. Mesh sensitivity study was done on the model to get better accuracy results and optimum computational load. The model involved internal space of the mosque and 160 prayers during the congregation prayers. It was discovered that, the particle spreading characteristics was found to be influenced mostly by the velocity distribution and velocity vector inside the mosque. This is due to force flow generated by fan and air conditioner air flow. Particles size less than 10  $\mu\text{m}$  were the most deposited on the wall and ceiling. The particles greater than 30  $\mu\text{m}$  deposited on the ground and the prayers body. The location of assailant at the center was found to cause the most infection among the prayers which was 52% of the total prayer with the  $R_0$  of 0.83. The assailant at top right and bottom right produced high  $R_0$  of 0.73 and 0.6 while top left produced the lowest which was 0.32. The existence of partition was found to reduce the particle spreading from the assailant at bottom left.

**Keywords:** Airborne, ventilation, pathogen, indoor, CFD

## 1. Introduction

COVID-19 outbreak were first reported in Wuhan, China and later spread throughout the world becoming a global pandemic <sup>1</sup>. The coronavirus was believed to be transmitted from animals to humans and later became a human-to-human transmission. As of June 29, 2021, the total confirmed cases globally are almost 181 million and almost 4 million deaths. It was believed that the coronavirus transmission to human started at a wet market in Wuhan, China <sup>2</sup>. While the research on Covid-19 has been done intensively, however, less attention has been focused on the possibility of the virus transmission through aerosol dispersion inside an enclosed space where people spent most of their time in indoor environment. Aerosols particles are smaller compared to respiratory droplets and have a significantly higher transmission distance and can remain in air for much longer period <sup>3</sup>. Respiratory viruses such as COVID-19 are believed to be transmitted through multiple ways such as physical contact with contaminated surface and respiratory droplet. There are two paths for the virus to spread through airborne which is a droplet transmission and aerosols transmission. The infected person will expelled the viral particles during breathing, talking, coughing and sneezing <sup>4</sup>. Respiratory particles can be distinguished by determining the size of the particles. Large respiratory droplet, with the size of particle of more than 100  $\mu\text{m}$  are likely to fall to the ground within 1 to 2 meter due to gravity. Small respiratory

\*Corresponding author: [mn.hidayat@utm.my](mailto:mn.hidayat@utm.my)

droplets which is typically 5  $\mu\text{m}$  or less can be categorized as aerosols, and can remain airborne for a long time, and the viruses attached to the droplet can remain viable for up to several hours<sup>5</sup>. Small droplets are also formed from the evaporation process of large droplet<sup>6</sup>. The expelled respiratory droplet was found to be able to travel as far as (7 - 8 m). The droplets from the coughing of the infected person will remain viable in the air to the people near 6 feet and 10 feet from the source in a static air environment.<sup>7</sup> Particles in the air are subjected to gravity, turbulent diffusion, inertial forces, thermal gradients, electromagnetic radiation.<sup>8</sup> Vapor pressure will be increased with high temperature and volatilization amount will be reduce with higher relative humidity<sup>5</sup>. 95% relative humidity will leads to higher deposition on the ground and human body and enhance the condensation effect of the particle<sup>7</sup>. The author also found that 40% relative humidity will have smaller droplet size due to the evaporation of water in the droplet which will cause the particle to suspend in the air for a longer period. There is a several characteristics of the particle that were exhaled from the mouth during the coughing process. During the event of coughing and sneezing, small respiratory droplets ranging from the size  $\sim 1 - 1000 \mu\text{m}$  were expelled from the nose and the mouth at velocities over 20 m/s for a period of 0.25 s with as much as  $\sim 40\,000$  droplets were expelled during sneezing and around 3000 droplets for coughing.<sup>5</sup> When cough jet interacts with the ambient air flow, the size of the particles will increase therefore reducing the velocity of the particle the more the particle travelled in the air<sup>9</sup>. Wang also found that droplets smaller than  $50\mu\text{m}$  are easier to be inhaled for the people of the same height as the infected person.

The location of source has a significant impact on the aerosol transport.<sup>10</sup> The study was conducted inside a classroom by using CFD simulation and found that student that was placed in the middle of the classroom transmitted  $\sim 2.1\%$  of exhaled particles to other student when compared to the student that was sit in front corner which exhaled  $\sim 0.55\%$  of  $1 \mu\text{m}$  aerosol particles to other students. The spreading of respiratory viruses increases when a person sneeze near the fresh air ducts in the car park.<sup>11</sup> The author found that respiratory particle concentration in underground car parks depend on the jet fan air velocity and when more than one person exists in the car park, the transmission of viral particle will significantly increase. The coughing from manikin near the inlet have higher overall inhaled aerosol by other manikin positioned inside the room when compared to coughing from manikin positioned further from inlet.<sup>12</sup> The aerosol inhalation was found the be three times more without the direct influence of air. The infection risk can be very low due to the existence of very high ventilation rate<sup>1</sup>. The author also found that the wind speed and wind direction have a significance toward the ventilation rate.

This paper aims to investigate aerosol particle spreading characteristic under transient state at different location released by an assailant, investigate the particle deposition according to the position of assailant and determine the virus reproductive number over time at different condition. The spreading during coughing process was validated with previous literature review using Computational Fluid Dynamics (CFD) simulation study. Mesh sensitivity study was done on the model to get better accuracy results and optimum computational load for the CFD simulation. The model involved in this study is the mosque and the prayers during the congregation prayers. The measurements of the mosque were taken to create geometrical model and the boundary condition involved in this study were taken from literature review.

## 2. Methodology

### 2.1 Geometrical Modelling

The geometry of the model is created by using FreeCAD software and mesh is generated by using scFlow student edition. The dimension for the prayers is based on the average size of Malaysian male which is 170 cm in height, 48.5 cm in width and 20.8cm in head length<sup>13</sup>. The size of the mouth is  $4 \text{ cm}^2$  based on the information extracted from<sup>5</sup>. The model of the prayers was arranged in the main hall as shown in the Figure 1. As much as 160 mannequins acting as prayers were arranged inside the main hall.

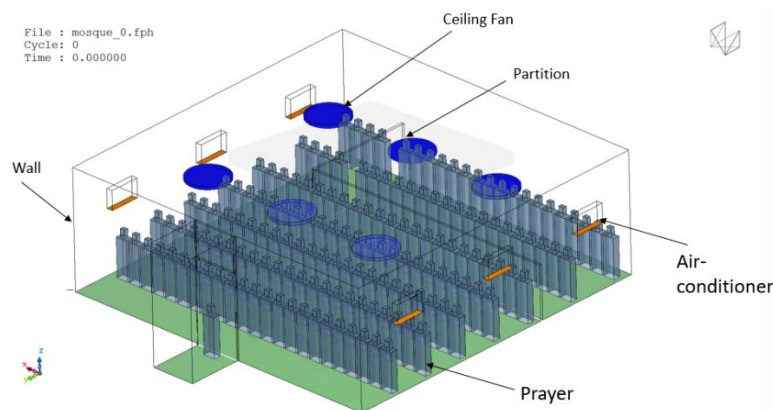


**Fig. 1 - Arrangement of prayers inside the main hall**

## 2.2 Governing Equation

For the air flow in this study, the governing equation that were used are conservation of mass, momentum, and energy. The equation for the governing equation is listed as below:

Conservation of Mass

$$\frac{\partial \rho}{\partial t} + \nabla \cdot (\rho v) = 0 \tag{1}$$

Conservation of Momentum

$$\rho \frac{\partial U_j}{\partial t} + \rho U_t \frac{\partial U_j}{\partial x_i} = \frac{\partial P}{\partial x_j} - \frac{\partial \tau_{ij}}{\partial x_i} - \rho g_j \tag{2}$$

Conservation of Energy

$$dU = \sigma Q - \sigma W + u' dM \tag{3}$$

The modelling of particle transportation can be done by analysis the forces acting on the particle. Thus, the equation of motion can be presented in Equation 4.  $\vec{u}_p$  is denoted as particle velocity vector and  $\vec{u}$  is represented by continuous-phase velocity. In the equation, it consists of 3 main forces component. The first force is drag force ( $F_D$ ), the second term refers to the gravitational force and finally external force denoted as  $\vec{F}$ .

$$\frac{d\vec{u}_p}{dt} = F_D(\vec{u} - \vec{u}_p) + \frac{\vec{g}(\rho_p - \rho)}{\rho_p} + \vec{F} \tag{4}$$

The drag force of the particle can be obtained from Equation 5. The change between particle velocity with continuous flow velocity multiple by the  $F_D$ .  $\mu$  is represented by dynamic viscosity,  $C_D$  is the drag coefficient and  $d_p$  is the particle diameter.

$$F_{drag} = F_D(\vec{u} - \vec{u}_p) = \frac{18\mu}{\rho_p d_p^2} \frac{C_D Re}{24} (\vec{u} - \vec{u}_p) \tag{5}$$

## 2.3 Mesh Sensitivity Study

After creating the geometrical model of the mosque and prayers, it was imported into scFLOW tool for meshing purposes and arranged as in the Figure 2. The reason why meshing is needed is because the governing equation cannot be applied to the arbitrary shape of the geometrical model. Meshing will allow the governing equation to be computed on a finite volume and predictable shaped. Mesh will affect the accuracy and the speed of the CFD simulation. For an ideal CFD results, the mesh should have an infinite number of cells. However, it is impossible to have an infinitely fine mesh, due to lack of computational power and the meshing will take a very long time. Therefore, fine mesh with finite number of cells will be compared to the ideal cases of infinitely fined mesh with infinite number of cells. However, there is always error involved in comparing the real mesh with ideal mesh. Mesh refinement study is used to estimate the discretization in error. The error can be calculated by using the Equation 6.

$$e_{21}^{extr} = \left| \frac{\varphi_1 - \varphi_0}{\varphi_0} \right| \tag{6}$$

Based on the Equation 6,  $e_{21}^{extr}$  represented the extrapolated error and,  $\varphi$  is the value that we want to find. Meshing near the mouth was set to 40 mm with growth rate of 1.2. The maximum size of the mesh is 400 mm as shown in the Figure 2. The meshes were categorized into several type, which is fine, medium, and coarse. Each type can be differentiated by their cell length and in this case, representative cell length,  $h$  was introduced. The value of  $h$  can be calculated by using the Equation 7.

$$h = \frac{1}{N} \sum_{Cells} V_p^{1/3} \tag{7}$$

Where  $h$  is the representative cell length,  $N$  is the number of cells and  $V$  is the volume. The importance of finding,  $h$  is because it signifies the average element size of the meshes which tells in which category the meshes in and it also can tell that when  $h$  approaching zero which is an infinitely fine mesh,  $N$  will become infinite. Celik, Zhang <sup>14</sup> suggest

that the grid refinement factor that can be found in Equation 8 should be greater than 1.3 or 30%. From the equation, the mesh convergent plot of fine, medium, and coarse were shown against the velocity in Figure 3.

$$r = \frac{h_{fine}}{h_{coarse}} \tag{8}$$

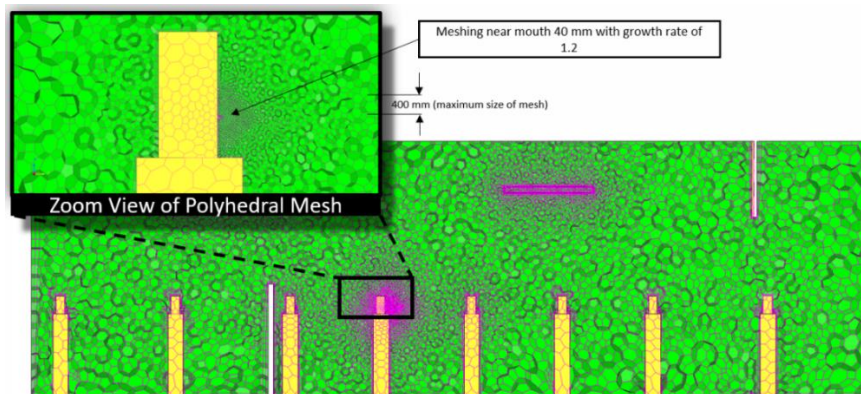


Fig. 2 - Cross sectional view of polyhedral mesh on the model

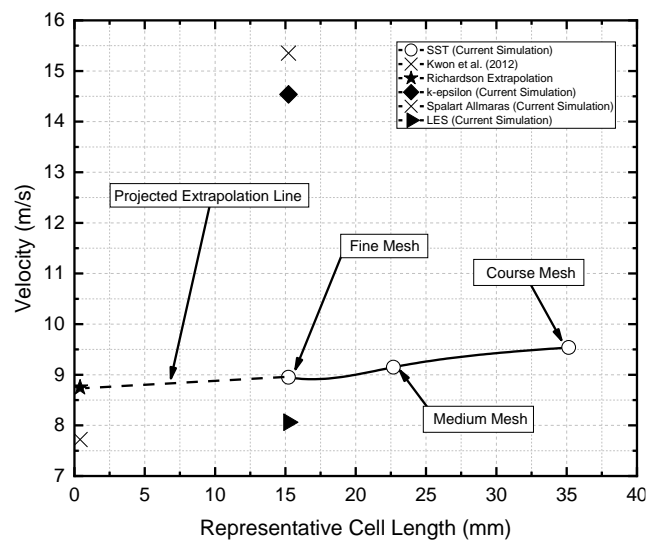


Fig. 3 - Mesh convergence plot for velocity

The axial velocity that was used in this study located at 1.6 m from the ground level. From Figure 3, the mesh sensitivity obtained were different for each mesh type. It is expected that fine mesh will be the most accurate among the other meshes therefore fine mesh was chosen as the boundary condition. The representative cell length for fine length is 15.22 mm with the value of 8.95 m/s, the values were obtained by running the CFD simulation with SST model. The values obtained from Grid Convergence Index were tabulated in Table 1. For Grid Convergence Index, the value of representative length was only taken when errors for fine mesh size is less than 5%<sup>15,16</sup>. The table shows the different mesh size, and the errors were compared to the value of representative length, h = 0.

Table 1 - Data obtained from the mesh sensitivity study

Mesh Size	Representative Length	Present Simulation (SST)	Relative Error
Infinitely small	0	8.67	Reference
Fine	15.22	8.95	3.18 %
Medium	22.68	9.15	5.49 %
Course	35.15	9.54	9.98 %

## 2.4 Selection of Turbulence Model

For this study, turbulent model was chosen in the CFD simulation since most flows are regarded as turbulent flows naturally. Four turbulent models that are commonly used were chosen in this study are SST k-omega, K-epsilon, Spalart Almaras, and Large Eddy Simulation (LES). The turbulence model used can also be seen from the Figure 3. For the simulation, velocity will be the output parameter. The values for velocity obtained from the simulation were compared to the velocity obtained by Kwon et al. (2012) experimentally which is 7.72. The selection of the turbulence model was based on the closest value to the experimental data where the LES model has the closest value to the experimental data which is 8.062.

## 2.5 Boundary Condition

The boundary condition, the values were obtained from the literature review. Ganegoda, Wijaya, Amadi, Erandi, Aldila<sup>17</sup> state that relative humidity and temperature will affect travelling distance of the respiratory droplets. He also states that that 3000 of particles were released during coughing with the peak velocity of between 10 m/s to 20 m/s with a mouth opening of 4 cm<sup>2</sup>. The boundary conditions that were set in this simulation were summarized in the Table 2.

**Table 2 - Boundary condition used in the study**

Parameter	Value
Analysis type	Transient
Type of Flow	Turbulence
Turbulent model	LES
Number of time step	1000
Time steps (adaptive)	0.1 s (begin)
Ambient & Inflow temperature	37 °C
Inflow humidity	100 %
Ambient humidity	50 %
Density of droplet particle	1000 kg/m <sup>3</sup>
Coefficient of Restitution	0.78
Number of particles	3000
Type of Particle Diameter	Gaussian
Average Velocity of Particle	11.2 m/s
Initial Particle Velocity	25 m/s

## 2.6 Experimental Validation

The velocity obtained from the simulation will be compared to the experimental value that were obtained from Kwon, Park, Jang, Cho, Park, Kim, Bae, Jang<sup>18</sup>. In this study, LES were chosen among the turbulence model due to the accuracy of LES which have the closest value of velocity when compared with the experimental value. The comparison of the data was tabulated in Table 3.

**Table 3 - Validation table**

Height (m)	u-velocity outlet (Kwon 2012)	u-velocity outlet (LES Present)	Relative error (%)
1.60	7.72	8.06	4.43%
1.65	9.68	10.03	3.62%
1.70	11.64	12.05	3.52%
1.75	13.60	14.25	4.78%
1.80	15.56	16.31	4.82%

## 3. Result

### 3.1 Particle Spreading Characteristic

The operating condition of the model consist of 5 main areas. The areas are the bottom left, bottom right, centre, top left, and top right of the mosque's main hall. The measurement of particle deposition is done on the assailant and 5 prayers near the assailant, the wall, ceiling, and the ground. The simulation is done based on the condition in the afternoon where the congregation prayers is usually done. The areas involved in the simulation are shown in Figure 4.

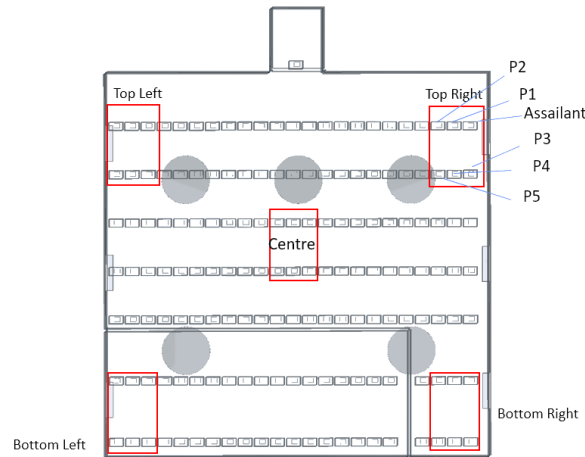


**Fig. 4 - Areas involved and the location of assailant**

The velocity distribution in horizontal inside the main hall of mosque is shown in Figure 5 and Figure 6. The measurement of the velocity distribution is taken at the middle of the prayer’s mouth and at time,  $t = 20s, 40s, 60s, 80s$  and  $100s$ . In the figure also shows the particle spreading from the assailant mouth over time. As the magnitude of velocity increases, the particle spreads further from the assailant and spreads throughout the mosque. The location of the assailant is at the top left of the mosque’s main hall. The plane is measured at the height  $1.63m$  from the ground which is the height from the ground to the middle of the assailant’s mouth which also applied to other areas. The highest velocity is  $2.85\text{ m/s}$  which can be seen mostly located at the middle area of the mosque. This is due to the middle area of the mosque are more exposed to the fan and air-conditioner when compared to other areas. The lowest velocity magnitude is  $0.15\text{ m/s}$ . The particle can be seen spreading actively after the 40 seconds. In the figure, particle is coloured in pink. The simulation is also being done at other assailant location inside the mosque based on Figure 7. The velocity vector is seen to be affected by the fan and the air-conditioner. The velocity vector is found to be higher in the middle part of the main hall when compared to the rest of the area. Figure 7 shows the velocity vector for different areas inside the mosque at time 100 seconds.

#### 4. Particle Deposition

The particle deposition in this simulation is measured at the ground, wall, ceiling, assailant body, prayer 1, prayer 2, prayer 3, prayer 4 and prayer 5. The location of prayers can be referred to Figure 8. The deposited particle is also measured at different location inside the mosque such as bottom left, bottom right, centre, top left and top right. The deposited particles are measure at time,  $t = 100s$ . Based on Figure 8, most of the particles are found to deposit on the ceiling. This is probably due to the small particle size ( $0 - 10\ \mu m$ ) that are light, and the effect of gravity is neglected. The particle deposition on the prayers is very small which is near 0. However, in Figure 8, some of the particle deposited on the prayers are regarded as 0 due to the rounding off the number to 2 decimal places. The reason behind this is probably due to the surface area of the prayers which is smaller when compared to ceiling and wall. The deposition on ground is small is due to the aerosol characteristic of the particle that causes the particle to linger in air longer. The number of particles deposited on the prayers in Figure 8(a) shows that prayer 4 and prayer 5 received more particles when compared to other prayers. prayer 3, 4 and 5 are in front of the assailant. However, prayer 3 received almost 0 particles due to the prayer location which is under the air-conditioner. This coincide with the finding from Nazari A. et al. (2021), where the safest location from the viral infection is near the inlet. The airflow from the air-conditioner is pushing the particles away from the prayer 3. In Figure 8(b) the particle deposition on the assailant body is high. This is probably due to the partition near the assailant which causes disruption on the local flow field. Based on Abuhegazy, Talaat, Anderoglu, Poroseva<sup>19</sup>, self-deposition increases on the student that is in the presence of the screen from 47% to 60% and the total aerosol transmission is significantly decreases which agrees with the finding where the deposition on assailant body is high when compared to other prayers due to the presence of partition near the assailant.

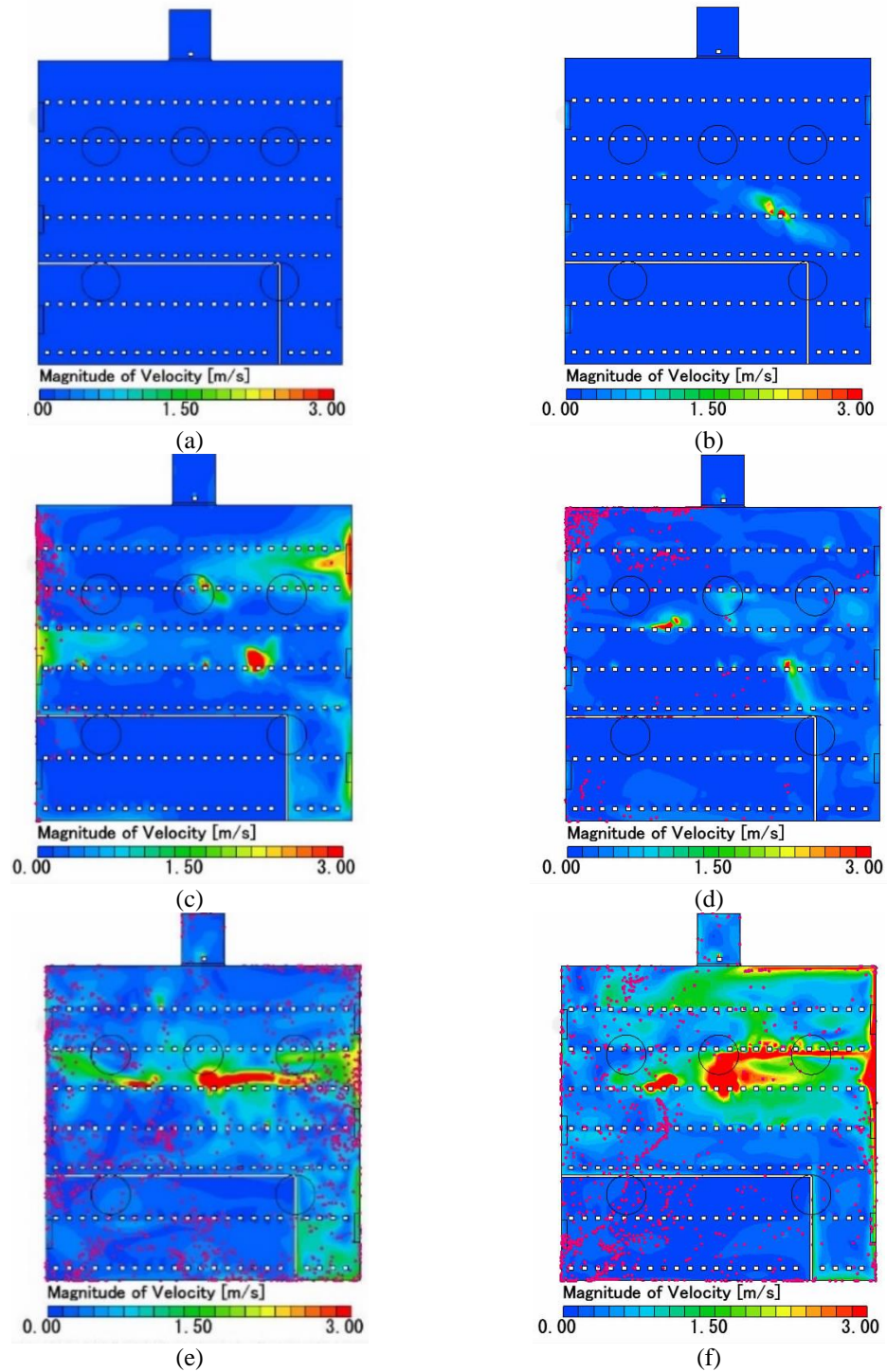


**Fig. 5 - The velocity distribution and the particle spreading observed at horizontal plane and the location of assailant at centre of the mosque at time (a) 0s; (b) 20s; (c) 40s; (d) 60s; (e) 80s and; (f) 100s**

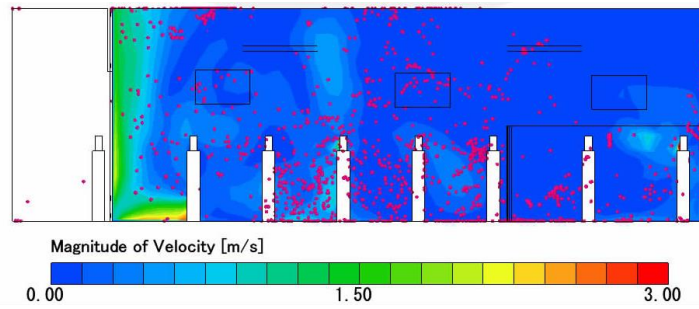


Fig. 6 -Velocity distribution for vertical plane at assailant position at bottom right of the mosque at time 100s

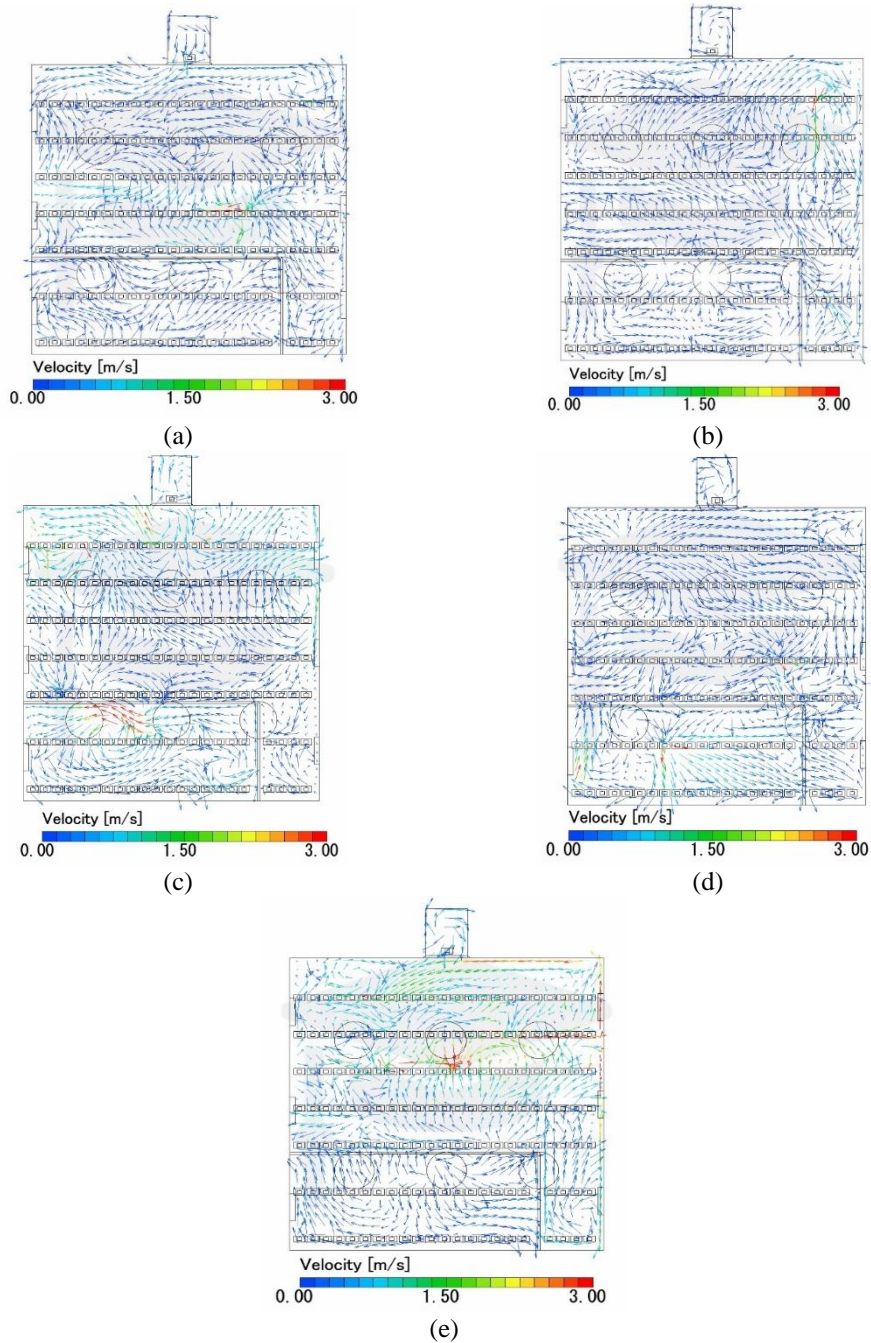
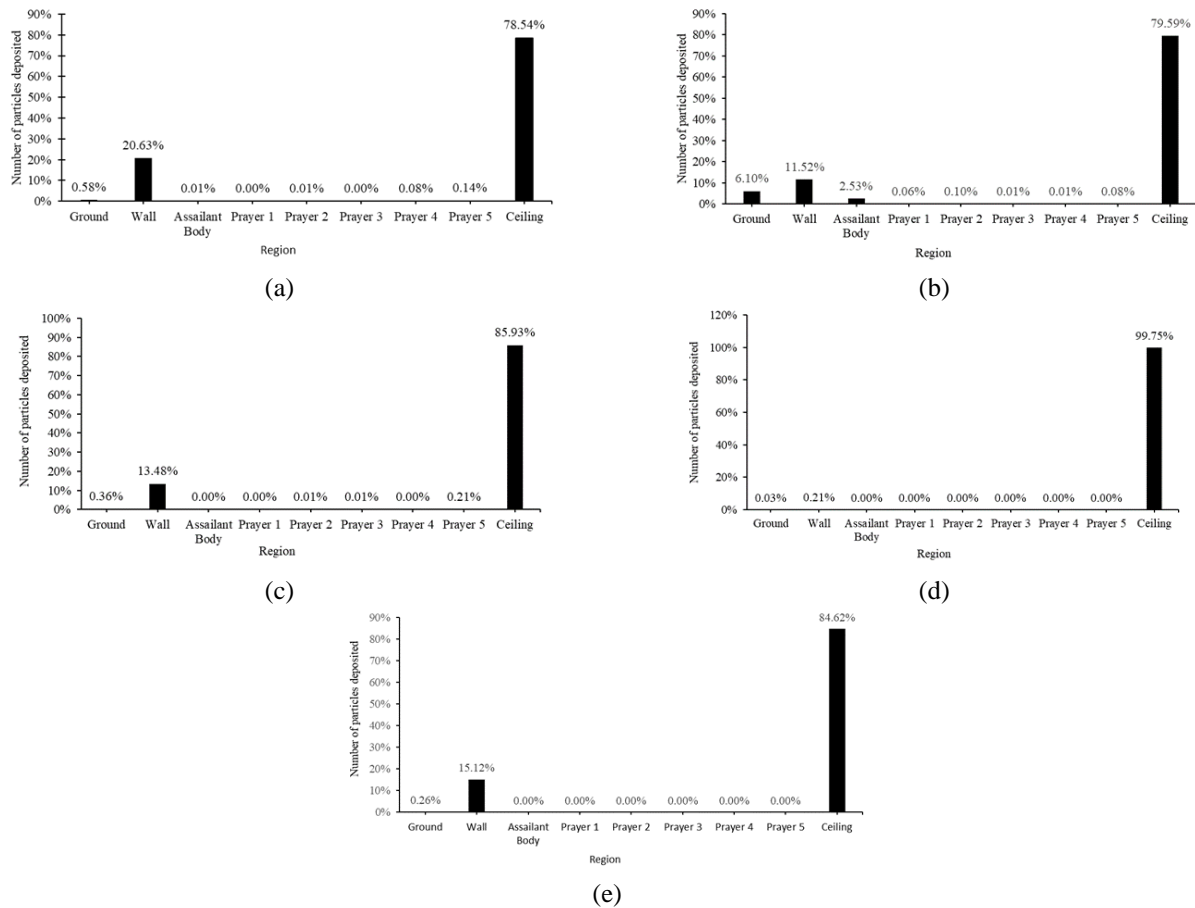


Fig. 7 - The velocity vector inside the main hall of the mosque at time,  $t = 100s$ , based on the assailant location inside the mosque (a) bottom left; (b) bottom right; (c) top left; (d) top right and; (e) centre





**Fig. 8 - Particle deposition on different region inside the mosque at the position of assailant at (a) bottom left; (b) bottom right; (c) centre; (d) top left and; (e) top right**

### 4.1 Virus Reproductive Number

The infection of the prayers is counted by assuming that the prayers will get infected if particle deposition are found on them. Based on Yan & Lan (2020), the cough containing virus concentration of  $4 \times 10^4$  units/m<sup>3</sup> will greatly increase the virus reproductive number. The particle spreading can be seen from Figure 9. Based on Figure 9, the number of infected prayers is counted based on the location of assailant from time,  $t = 0$  seconds until 100 seconds. The total number of prayers inside the mosque is 160. The virus reproductive number is calculated by using the equation 9.

$$R_o = \beta/\gamma \tag{9}$$

Where  $\beta$  is the number of infected and  $\gamma$  is the mean infectious period <sup>20</sup>, and in this case it is 100 seconds. From Figure 9 we can obtain the number of infected prayers,  $\beta$  thus  $R_0$  can be calculated. The  $R_0$  for bottom left area is 0.45, bottom right is 0.60, top left is 0.32, top right is 0.73 and centre is 0.83. This shows that if an infected person coughs at the bottom left, top right, and centre of the mosque, it may cause higher infection among the prayers.

### 4.2 Comparison with Existing Paper

The data obtained from the particle deposition are compared with the finding from Abuhegazy, Talaat, Anderoglu, Poroseva <sup>19</sup>. In his paper, the effect of source location is found to have effect on the total aerosol’s transmission inside the classroom. The paper found that student sit at the back corner and front corner of the class, will result in increased deposition on the wall and ceiling by 44%. Student that sits at the centre back of the classroom will received the most particle self-deposition. This result is obtained in the current simulation where the particle deposition is high at ceiling and wall at the location bottom right and top left of the mosque.

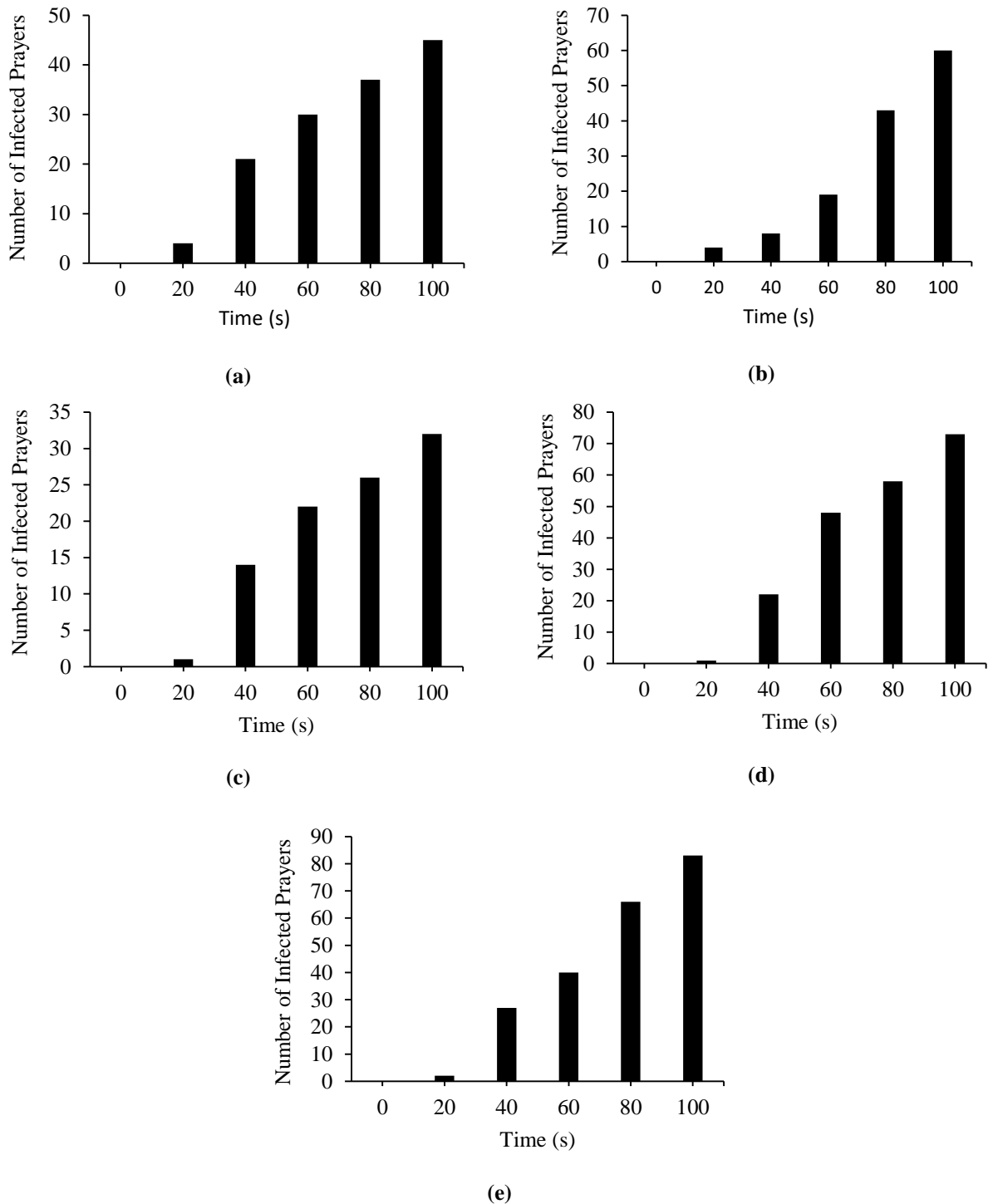


**Fig. 9 - Number of infected prayers over time at assailant’s location (a) bottom left; (b) bottom right; (c) top left; (d) top right and; (e) centre**

### 4.3 Practical Application

The super spreader event will occur when a huge amount of people gathered at the same place in a confined place. This can be seen from Figure 6 where a single person cough will infect as much 148 prayers out of 160 prayers in the mosque. It can be said that almost everyone in the mosque will be infected by the cough of an infected person. This can be seen from the Therefore, avoiding gathering in a confined space will reduce the chance of super spreader event. The areas at the bottom left, centre and top right of the mosque should be leave vacant based on the high number of infections from those areas after time,  $t = 100s$  that can be seen from Figure 6. The existence of partition inside the mosque can also be useful in reducing the particle spreading which can be seen from Figure 6(b), where the number of infected prayers is less than 100 after 100 seconds. This finding is with the agreement with Abuhegazy, Talaat,

Anderoglu, Poroseva <sup>19</sup>. where the installation of screen or barrier inside the classroom may reduce the total aerosol transmission from the source student by up to 92%.

#### 4.4 Limitation Finding

The time constraint and lack of computational power are proven to be a major limitation in doing this simulation. Due to lack of computational power, the simulation is only based on five different areas inside the mosque main hall and the particle deposition is only calculated on the five nearest prayers to the assailant which may affect the accuracy of the finding. The virus reproductive number in this study is determined by assuming that the prayers will be infected as soon as the aerosols particle deposited on their body. This, however, does not represent the real-world scenario where the person will only get infected if their antibody fails to eliminate the pathogen and the time for a person to show a symptom may take hours or days instead of 100 seconds.

#### 5. Conclusion

The study on the particle spreading characteristics, particle deposition and virus reproductive number over time at different location inside the mosque has successfully been done. The first conclusion is that the velocity distribution and velocity vector does affect the particle spreading characteristics throughout the mosque. The particles are found to be concentrated at the area with high velocity region which is usually found in the middle of the mosque due to the presence of fans and air-conditioner. The second conclusion is that the particle deposition is dependent on the particle size where the particle with smaller size (0 -10  $\mu\text{m}$ ) will be usually found deposited on the ceiling and walls and the particle with bigger size will be found deposited on the ground (> 30  $\mu\text{m}$ ). The aerosol particle deposition found on the body of the prayers are small when compared to the particle deposition on the wall and ceiling which is due to the small surface area of the prayers. The third conclusion is that the virus reproductive number are found to be high when the assailant is located at the top right, centre and bottom left of the mosque with the  $R_0$  value of 1.48, 1.47 and 1.34 respectively. The high amount of  $R_0$  will cause more prayers to be infected. The presence of partition inside the mosque can also be beneficial towards the prayer. This can be seen from the  $R_0$  value at bottom right which is 0.89. While the study focuses on the effect of location of assailant towards the particle reproductive number, the effect of location of ventilation is also important especially towards the air flow inside the mosque which will affect the particle spreading, particle deposition and the virus reproductive number.

#### Acknowledgments

This research was sponsored by Ministry of Higher Education (MOHE) through Fundamental Research Grant Scheme (FRGS/1/2021/TK0/UTM/02/98).

#### References

- [1] Liu Y-C, Kuo R-L, Shih S-R. (2020) COVID-19: The first documented coronavirus pandemic in history. *Biomedical journal*.43(4):328-333.
- [2] Mizumoto K, Kagaya K, Chowell G. (2020). Effect of a wet market on coronavirus disease (COVID-19) transmission dynamics in China. *International Journal of Infectious Diseases*. 2020;97:96-101.
- [3] Mat MNH, Basir MFM, Yusup EM. (2021). Fans deactivation for minimisation of airborne pathogen transmission: During Malaysians congregational prayer gathering in mosque. *International Communications in Heat and Mass Transfer*.129:105694.
- [4] Jayaweera M, Perera H, Gunawardana B, Manatunge J. (2020). Transmission of COVID-19 virus by droplets and aerosols: A critical review on the unresolved dichotomy. *Environmental research*. 109819.
- [5] Ho CK. (2021).Modeling airborne pathogen transport and transmission risks of SARS-CoV-2. *Applied mathematical modelling*. 95:297-319.
- [6] Parienta D, Morawska L, Johnson G, et al. (2011). Theoretical analysis of the motion and evaporation of exhaled respiratory droplets of mixed composition. *Journal of aerosol science*. 42(1):1-10.
- [7] Feng Y, Marchal T, Sperry T, Yi H. (2020). Influence of wind and relative humidity on the social distancing effectiveness to prevent COVID-19 airborne transmission: A numerical study. *Journal of Aerosol Science*. 147:105585.
- [8] Jayaweera M, Perera H, Gunawardana B, Manatunge J. (2020). Transmission of COVID-19 virus by droplets and aerosols: A critical review on the unresolved dichotomy. *Environ Res*. 188:109819.
- [9] Wang H, Li Z, Zhang X, Zhu L, Liu Y, Wang S. (2020). The motion of respiratory droplets produced by coughing. *Physics of Fluids*. 32(12):125102.
- [10] Abuhegazy M, Talaat K, Anderoglu O, Poroseva SV. (2020). Numerical investigation of aerosol transport in a classroom with relevance to COVID-19. *Phys Fluids*. 32(10):103311.
- [11] Nazari A, Jafari M, Rezaei N, et al. (2021). Effects of High-speed Wind, Humidity, and Temperature on the Generation of a SARS-CoV-2 Aerosol; a Novel Point of View. *Aerosol and Air Quality Research*. 21(8):200574.

- [12] Morawska L, Tang JW, Bahnfleth W, et al. (2020). How can airborne transmission of COVID-19 indoors be minimised? *Environment International*. 142:105832.
- [13] Deros BM, Mohamad D, Ismail AR, Soon OW, Lee KC, Nordin MS. (2009). Recommended chair and work surfaces dimensions of VDT tasks for Malaysian citizens. *European Journal of Scientific Research*. 34(2):156-167.
- [14] Celik I, Zhang W-M. (1995). Calculation of numerical uncertainty using Richardson extrapolation: application to some simple turbulent flow calculations.
- [15] Kamar HM, Wong KY, Kamsah N. (2020). The effects of medical staff turning movements on airflow distribution and particle concentration in an operating room. *Journal of Building Performance Simulation*. 13(6):684-706.
- [16] Wong KY, Haslinda MK, Nazri K, Alia SN. (2019). Effects of surgical staff turning motion on airflow distribution inside a hospital operating room.
- [17] Ganegoda NC, Wijaya KP, Amadi M, Erandi K, Aldila D. (2021). Interrelationship between daily COVID-19 cases and average temperature as well as relative humidity in Germany. *Scientific reports*. 1(1):1-16.
- [18] Kwon S-B, Park J, Jang J, et al. (2012). Study on the initial velocity distribution of exhaled air from coughing and speaking. *Chemosphere*. 87(11):1260-1264.
- [19] Abuhegazy M, Talaat K, Anderoglu O, Poroseva SV. (2020). Numerical investigation of aerosol transport in a classroom with relevance to COVID-19. *Physics of Fluids*. 32(10):103311.
- [20] Razak FA, Zamzuri ZH. (2021). Modelling Heterogeneity and Super Spreaders of the COVID-19 Spread through Malaysian Networks. *Symmetry*. 13(10):1954.